A Comparative Study of Different Feature Extraction Methods for Motor Imagery EEG Decoding within the Same Upper Extremity

Conference Paper · November 2018

DOI: 10.1109/CAC.2018.8623624

6 authors, including:

Yaqi Chu
Chinese Academy of Sciences
13 PUBLICATIONS **94** CITATIONS
SEE PROFILE

Xingang Zhao
Shenyang Institute of Automation Chinese Academy of Sciences
156 PUBLICATIONS **1,033** CITATIONS
SEE PROFILE

Peter Xu
University of Auckland
285 PUBLICATIONS **2,771** CITATIONS
SEE PROFILE

Yiwen Zhao
New Jersey Institute of Technology
89 PUBLICATIONS **1,686** CITATIONS
SEE PROFILE

A Comparative Study of Different Feature Extraction Methods for Motor Imagery EEG Decoding within the Same Upper Extremity

Yaqi Chu[1, 2, 3], Xingang Zhao[1, 2], Yijun Zou[1, 2, 3], He Zhang[5], Weiliang Xu[1, 4], and Yiwen Zhao[1, 2]

[1]*State Key Laboratory of Robotics, Shenyang Institute of Automation (SIA),*
Chinese Academy of Sciences (CAS)
Shenyang, Liaoning, 110016, China
{chuyaqi, zhaoxingang, zouyijun, zhaoyw}@sia.cn
[2]*Institutes for Robotics and Intelligent Manufacturing,*
Chinese Academy of Sciences (CAS)
Shenyang, Liaoning, 110016, China
[3]*University of Chinese Academy of Sciences (UCAS)*
Beijing, 100049, China
[4]*Department of Mechanical Engineering*
University of Auckland
Auckland, 1142, New Zealand
p.xu@auckland.ac.nz
[5]*Department of Orthopedics, Xinqiao Hospital*
Third Military Medical University
Chongqing, 400038, China
alaflam@163.com

***Abstract*—Compared to other electroencephalogram (EEG) modalities, motor imagery (MI) based brain-computer interfaces (BCIs) can provide more natural and intuitive communication between human intentions and external machines. However, this type of BCI depends heavily on effective signal processing to discriminate EEG patterns corresponding to various MI tasks, especially feature extraction procedures. In this study, a comparison of different feature extraction methods was conducted for EEG classification of imaginary movements within the same upper extremity. Unlike traditional MI tasks (left/right hand), six imaginary movements from the same unilateral upper extremity were proposed and evaluated, including elbow flexion/extension, forearm supination/pronation, and hand grasp/open. To tackle the classification challenge of MI tasks within the same limb, four types of feature extraction methods were implemented and compared in combination with support vector machine (SVM) and linear discriminant analysis (LDA) classifiers, such as wavelet transformation, power spectrum, autoregressive model, common spatial patterns (CSP) and variants of filter-bank CSP (FBCSP), regularized CSP (RCSP). The overall accuracies of the CSP were significant higher than other three types of feature extraction on a dataset collected from 8 individuals, particularly the SVM with FBCSP had the best performance with an average accuracy of 71.78%. These decoding results of MI tasks during single upper extremity are encouraging and promising in the context of more natural MI-BCI for controlling assisted devices, such as a neuroprosthetic or robotic arm for motor disabled individuals with highly impaired upper extremity.**

***Keywords*—Brain-computer interface, motor imagery EEG, same upper extremity, feature extraction, common spatial patterns.**

This work was supported by the Nation Natural Science Foundation of China (Grants nos. 61503374 and 61573340), and in part by the Frontier Science research project of the Chinese Academy of Sciences (Grant No. QYZDY-SSW-JSC005).

I. INTRODUCTION

Non-invasive brain-computer interfaces (BCIs) based on electroencephalogram (EEG) provide a promising pathway for the development of an interactive control of a robotic device or a neural prosthesis to assist motor disabled persons [1, 2], especially for the EEG modality of motor imagery (MI) [3, 4]. MI-based BCIs decode a specific mental activity into control command by power modulations of sensorimotor rhythms, such as the event-relayed de/synchronization (ERD/ERS) activity [5, 6]. Compared to steady-state visual evoked potential (SSVEP) [7] or P300, the MI-based BCIs are more useful and flexible in view of natural and intuitive interaction.

A variety of MI-based BCIs were developed in different fields, such as control of wheelchairs [8], prosthetic arms or devices [9], mobile and humanoid robots [10], mind-driven navigation in gaming or virtual reality [11]. However, most MI-based BCIs can only discriminate a finite number of MI tasks (usually two or three) and decode spatially well separated MI patterns in brain areas as control commands. For example, left/right hand, foot and/or tongue MI tasks are the most commonly adopted among the MI-based BCI systems [6, 12]. Due to the fact that MI tasks within the same upper extremity activate and occupy the same brain regions on the motor cortex area [13, 14], the EEG signals have non-stationary and overlapped representations, which makes them really challenging to detect the MI tasks from the same limb.

There are relatively few researches that address the classification challenge of MI tasks from the same limb. Vuckovic and Sepulveda combined time-frequency features and an Elman neural network to detect four real and imaginary wrist movements (flexion/extension and pronation/supination), with 71.3% accuracy for each pair [15, 16]. Similarly, Edelman *et al.* adopted band power features and source space analysis to improve the decoding performance of imaginary wrist movements with an average accuracy of 81.4% [17]. Liao *et al.* applied power spectral features and a support vector machine (SVM) classifier to decode ten pairs of finger movements from one hand using EEG signals [18]. Menon *et al.* conducted a preliminary comparison of nine various schemes to decode rest against two MI tasks within the same limb (hand grasp and elbow), using three state-of-the-art feature extraction methods with an average accuracy of 58.4% [14]. In a further study, a decoding scheme of integrating time-domain features with optimized SVM was proposed to improve the performance of 3-class BCI with 74.2% accuracy, including autoregressive (AR) model coefficients, waveform length (WL) and root mean square (RMS) [19]. Ofner *et al.* investigated the decoding of executed/imagined movements of single upper limb from the time-domain of low-frequency EEG, with accuracy of 55% for executed movements, 27% for imagined movements [20]. From the above studies, we can see that the decoding accuracy and feasibility of the MI-based BCIs highly relies on EEG signal processing for the different MI tasks within the same limb, particularly feature extraction procedures.

In view of EEG signals have relative low spatial resolution and signal-to-noise ratio, an effective signal processing scheme is extremely important. Furtherly, the feature extraction has a direct impact on the performance of a classifier. Currently, massive feature extraction methods and classifiers have been developed and applied to EEG recognition for MI-based BCIs [21, 22]. Some widely used feature extraction methods have been implemented in the traditional MI tasks (left/right hand), including power spectral analysis [23], wavelet transformation [24], AR model [25], common spatial pattern (CSP) and variants of filter-bank CSP (FBCSP), regularized CSP (RCSP), sub-band CSP (SBCSP) [26]. However, for the MI tasks within the same limb, there are few comparison studies by using those state-of-the-art feature extraction methods.

In this paper, a comparative study for decoding multiple MI tasks within the same limb was evaluated by combining four types of feature extraction methods with SVM and linear discriminant analysis (LDA), including wavelet transformation, power spectrum, AR model, and CSP (FBCSP, RCSP). Six imaginary movements from the same upper extremity were designed, including elbow flexion/extension, wrist or forearm supination/pronation, hand open/close (similar to [20]).

The overall structure of this paper are organized as follows. The systematic framework for MI decoding is introduced in Section II. The MI experiment and datasets are presented in Section III. Section IV describes detailed signal processing methodology. Then, experimental results and discussions are showed in Section V. Finally, Section VI gives the conclusions and future works.

II. Overall Decoding Framework

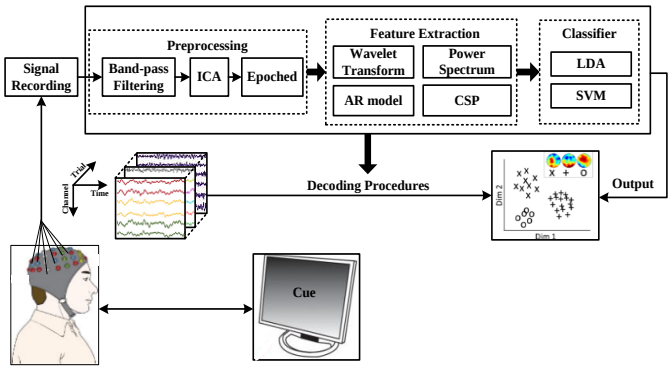

Fig. 1. The overall decoding framework for various MI EEG signals by using different feature extraction methods and classifiers.

The theme of our study is to compare the performance of different feature extraction methods for decoding MI EEG elicited by the same upper extremity. The schematic diagram of the overall decoding scheme is illustrated in Fig. 1, which mainly includes three procedures: preprocessing for raw EEG, four types of feature extraction methods and two classifiers. The raw EEG signals was recorded by the way of non-invasive wet electrodes when subjects do diverse imaginary movements within the same limb. The preprocess procedure was adopted to construct pure MI EEG datasets, including band-pass filtering, independent component analysis (ICA), and sliding windows segmentation. Different domains of features were retrieved by power spectrum (frequency domain), AR model (time domain), wavelet transform (time-frequency domain) and CSP (spatial domain). The extracted features were separately fed to SVM and LDA to discriminate the various MI tasks within the same limb. The results were comparatively evaluated and analyzed in the aspect of feature extraction and classifier individually.

III. Motor Imagery EEG Datasets

A. Subjects

Eight right-handed individuals (all males, mean age 25 years, range 25-28 years, numbered S01-S08) with thin hair were recruited to participate the MI experiments. All individuals were healthy, without any disease history of neurological or cognitive disorders. Explicitly, none of them has any previous experience of the MI-BCI experiment. Written informed consent was signed, and the experiment was approved by the ethics committee of the Third Military Medical University.

B. Experimental Paradigm

According to [20], six imaginary movements (shown in Fig. 2) from the same limb were designed for three joints (elbow, wrist and hand). In the condition of electromagnetic shielding, the participants sat in a comfortable chair with armrests and watched a screen from a distance of about 1 m. The experimental paradigm was trial-based and cues were displayed on the screen. Before the experiment, all movements started at a neural position: the hand half open, the forearm extended to 120 degrees and in a neutral rotation, i.e. thumb on the inner side.

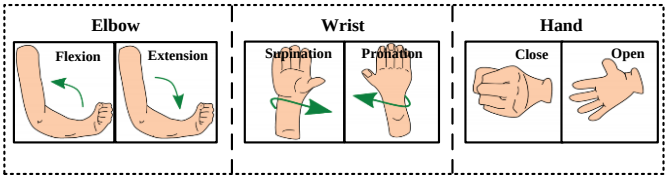

Fig. 2. The diagram of six imaginary movements within the same limb.

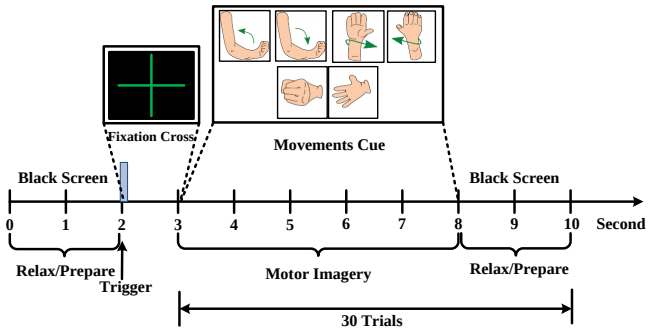

Fig. 3. The motor imagery EEG paradigm.

The experiment consists of 10 sessions with the total duration of one hour. All sessions were implemented during the same condition with a break of ten minutes between the two consecutive sessions. Figure 3 shows the sequence of the paradigm in a session. The first 2 s was a relax/prepare state with a black screen. Subsequently, a fixation green cross was shown at the center of the screen with duration of 1 s to indicate the beginning of one trial. Immediately, a movement cue (a figure in Fig. 2) displayed on the screen with duration of 5 s. In this period, the individual was instructed to respectively perform relevant MI tasks according to the cue, such as repeatedly imaginary kinesthetic grasp of hand. In addition, to minimize the artefacts that may arise by the subjects, the participants were asked to limit their body movements and try not to blink or swallow during the MI period. At the end of the trial, the subjects perform relax/prepare state and hold back to the neutral position. Each of the cues was presented by a randomized order. In every session, we recorded 30 trials with 5 trials per class. For each subject, there are total 300 trials of MI tasks with 5 s length in an experiment.

C. Recording and Dataset

The EEG were recorded using a grid cap with 64 Ag/AgCI scalp electrodes provided by Plexon Inc., USA. The electrodes were arranged according to the international 10-20 positioning system. The left mastoid electrode was adopted as reference channel and the right mastoid electrode served as ground. The original analog signals were transformed by OmmiPlex Neural Data Acquisition System, including pre-amplification, analog-to-digital conversion, and a low-pass filter. An additional notch filter with 50 Hz was applied to eliminate the power line artefacts. The EEG were sampled at 1 kHz and saved in the form of channels×times×trials with 64×5000×300. To obtain most representative MI EEG, a 4 s period was cut out from each trial. Hence, the datasets were formed by a three-dimensional array of size 64×4000×300 for each subject. The datasets were randomly divided into 75% training datasets and 25% testing datasets.

IV. Decoding Methodology

A. EEG Preprocessing

To eliminate the unwanted parts of the EEG segments, the preprocessing procedure was applied, including a) band-pass filtering, b) ICA and c) sliding windows segmentation.

1) Band-pass filtering: For MI EEG, the phenomenon of ERS/ERD obviously appears in the frequency range of mu (8-12 Hz) and beta (18-26 Hz) rhythms [6]. Hence, the 8-30 Hz frequency band possesses the most discriminative information related with MI tasks. In this study, a fifth-order Butterworth band-pass filter with cutoff frequency of 8 Hz and 35 Hz was applied to attenuate the frequency component of specific noises while amplify interested frequency band. After signal filtering, a large part of noise can be removed, such as EMG (higher than 35 Hz) and electrical line interference (50-60 Hz).

2) ICA: To remove EOG, an ICA procedure was adopted. The EEG signals were decomposed into multiple independent components (ICs) based on high order statistics. By visual inspection, some ICs corresponding to EOG artefacts were rejected. The selected non-artefactual ICs were mixed and projected back onto the original channel space to obtain the EOG-free EEG signals. In this study, 32 ICs were isolated from EEG signals for each subject by using FastICA algorithm of the EEGLAB software [27].

3) Sliding windows segmentation: For recorded EEG, we just only focus on the segments of MI period. Moreover, a trial of MI tasks need repeatedly imagine limb movements for a certain time to generate stable and effective rhythm modulation during brain activity. To improve the temporal resolution of EEG, a sliding window was used to split trial-based EEG into overlapped segments. In this study, a four-second period of motor imagery was divided into 16 segments of 1 s length with 0.2 s step size by the 1 s sliding window with 80 % overlap. Hence, for each subject, the dataset was 64×1000×4800, where 4800 was the number of epoch signal.

B. Different Feature Extraction Methods

The core of a MI-based BCI system is feature extraction, which is used to highlight important information corresponding to MI and eliminate non-informative parts. To compare the performance, four types of feature extraction methods were adopted, including AR model, power spectrum, wavelet transform and CSP. A MI EEG segment is denoted by $\boldsymbol{X} \in R^{C\times N}$, where C is the number of channels and N is the length of signal. For each channel, the signal series were denoted by eeg_t, where $t = 1, 2, ..., N$.

1) AR model: The classical AR model is a time-domain analysis method, which depicts time-varying features of EEG signals. AR model provides information regarding previous samples by a weighted linear combination of samples in a segment. The time resolution and accuracy of AR model depend on the length of the signal segment. A shorter length can bring a higher resolution and result in a larger estimation error of the model. To solve the problem, an adaptive AR (AAR) model was used in this paper. The mathematical formula of AAR model is given as follows:

$$eeg_t = \alpha_{1,t} eeg_{t\text{-}1} + \alpha_{2,t} eeg_{t\text{-}2} + \cdots + \alpha_{p,t} eeg_{t\text{-}p} + \varepsilon_t, \quad (1)$$

where $\alpha_{i,t}$ ($i = 1, \ldots, p$) are AAR model coefficients, p is the model order ($p = 4$ in this study) and ε_t is the white noise. The 4 model coefficients estimated by a recursive least square (RLS) algorithm were used to represent the EEG features.

2) Power spectrum: The power spectrum method is mainly used to extract band energy features, which represent the ERD/ERS variation in the frequency domain. The power features can be obtained by a direct method (fast Fourier transform, FFT). However, since the EEG signal is non-periodic, the FFT estimation cannot conform consistent estimation condition and readily generate spectrum leakage. In this study, the welch method was used to estimate the frequency spectrum. For MI EEG mostly located in 8-30 Hz, four sub-bands with bandwidth of 6 Hz were divided, including alpha (8-13 Hz), sigma (13-18 Hz), low beta (18-23 Hz) and high beta (23-28 Hz) rhythms. For each channel, the power spectral features of each sub-band were computed by averaging powers within the frequency range using welch method.

3) Wavelet transform: The wavelet transform provides an effective solution for non-stationary EEG signal to extract time-frequency features. Moreover, the discrete wavelet transform (DWT) can produce fine temporal and spectral analysis by using different contracted and dilated versions of the wavelet base. The DWT decomposes signals into detailed and approximate coefficients by successive high pass and low pass filtering created by orthonormal wavelet bases. These coefficients span different non-overlapping sub-bands for the EEG signals. In this study, a 2-level DWT with gabor wavelet was adopted to divide the 8-30 Hz MI EEG into four sub-bands, including 8-13.5 Hz, 13.5-19 Hz, 19-24.5 Hz and 24.5-30 Hz. The power features were computed by averaging the sum of the signals reconstructed from the coefficients within each sub-band.

4) CSP: The common spatial pattern (CSP) is an effective spatial filter to extract features for discriminating two classes of EEG signals related to MI tasks. For two classes of MI EEG, $\boldsymbol{x}_j^k \in \boldsymbol{X}$ denotes the *j*-th EEG segment from the k class ($k = 1, 2$). The corresponding spatial covariance matrix $\sum$ is computed by

$$\sum_k = \frac{1}{N_k} \sum_{j=1}^{N_k} \boldsymbol{x}_j^k (\boldsymbol{x}_j^k)^T, \quad (2)$$

where N_k is the number of EEG segments in class k. The spatial filters of CSP are learned and computed by maximizing the following ratio function:

$$\max_{\boldsymbol{w}} \mathbf{J}(\boldsymbol{w}) = \frac{\boldsymbol{w}^T \sum_1 \boldsymbol{w}}{\boldsymbol{w}^T \sum_2 \boldsymbol{w}} \quad s.t. \quad \|\boldsymbol{w}\|_2 = 1, \quad (3)$$

where $\boldsymbol{w} \in \boldsymbol{R}^C$ is a spatial matrix, and $\|\bullet\|_2$ represent l_2-norm. By solving the generalized eigenvalue decomposition problem, the relevant eigenvectors can be obtained to form $\boldsymbol{w}$.

$$\sum_1 \boldsymbol{w} = \lambda \sum_2 \boldsymbol{w} \quad (4)$$

Generally, the *e* eigenvectors corresponding to the highest and the lowest eigenvalues are selected to construct spatial filtering matrix $\tilde{\boldsymbol{w}} \in \boldsymbol{R}^{C \times S}$, $S = 2 \times e$. The projection of a given EEG $\boldsymbol{X}$ is given by

$$\boldsymbol{Z} = \tilde{\boldsymbol{w}}^T \boldsymbol{X}. \quad (5)$$

Then the spatial feature vector is formed as $\boldsymbol{f} = [f_1, \ldots, f_S]$ by

$$f_m = \log\left(\frac{\mathrm{var}(\boldsymbol{Z}_m)}{\sum_{m=1}^{S} \mathrm{var}(\boldsymbol{Z}_m)} \right), \quad (6)$$

where $\mathrm{var}(\bullet)$ and $\log(\bullet)$ denote the variance, logarithm operator respectively.

Due to the CSP for solving two class problem, a One-vs-Rest strategy was applied to cope with multi-class MI EEG. In this study, for six MI classes, there were six CSP filters. For each CSP, the number of selected eigenvectors is *e* = 2. Hence, the total spatial filtering matrix is $\boldsymbol{W} \in \boldsymbol{R}^{C \times S}$, where $S = 2 \times e \times 6$ is the number of CSP projections. In addition, FBCSP and RCSP were also introduced in the comparison study. For FBCSP, three frequency bands 8-16 Hz, 17-25 Hz, and 26-32 Hz were separately used to filter EEG. In summary, for each EEG epoch, 24, 72, and 24 spatial features were extracted for CSP, FBCSP, and RCSP, respectively.

C. Classification

Considering the performance and computation complexity, two efficient state-of-the-art classifiers (LDA and SVM) were used in this paper.

1) LDA: The commonly adopted classifier in BCI systems is the LDA, which aims to find a linear hyperplane to characterize or separate two classes of MI EEG signals. More explicitly, this hyperplane or projection is optimized by maximizing inter-class divergence and minimizing intra-class divergence synchronously. Since LDA is a binary classifier, a One-vs-One strategy was conducted to address multiple class classification. In this paper, the class of MI EEG was assigned using a maximum voting way from 15 LDA classifiers.

2) SVM: The SVM executes in a similar manner with LDA, by attempting to search a high-dimensional hyperplane to discriminate samples with a maximum margin. The generalization capabilities of the SVM are increased by maximizing this margin. The hyperplane can be obtained by solving the following optimization problem:

$$\min_{\mathbf{W},\mathbf{b}} \frac{1}{2}\|\mathbf{W}\|^2 + c\sum_{i=1}^{N} \zeta_i \quad s.t.: y_i(\mathbf{W}^T x_i + \mathrm{b}) \geq 1 - \zeta_i, \zeta_i \geq 0 \quad (7)$$

where c is a regularization term, ζ_i are slack parameters, x_i is the feature vector representing a sample, y_i is the associated label, i is the sample index. With the use of a kernel function which mapped the sample to higher dimensional space, an optimized hyperplane can be used to easily separate the mapped sample. In this study, a radial basis function (RBF) was selected as the kernel function. The kernel parameter and regularization

term c were optimized by a grid search in the range of (0, 5). Furthermore, a 5-fold cross-validation procedure was used to prevent over-fitting for training a classifier.

V. Experiment Results and Discussions

A. Comparison with different feature extraction methods

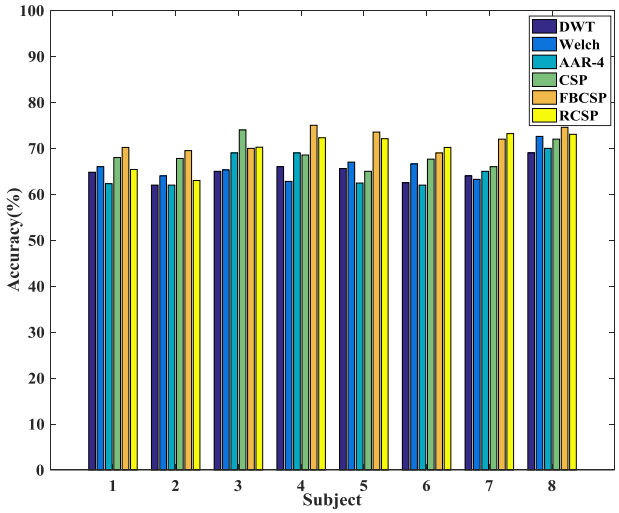

Fig. 4. The accuracy of SVM with different feature extraction methods for eight subjects, respectively.

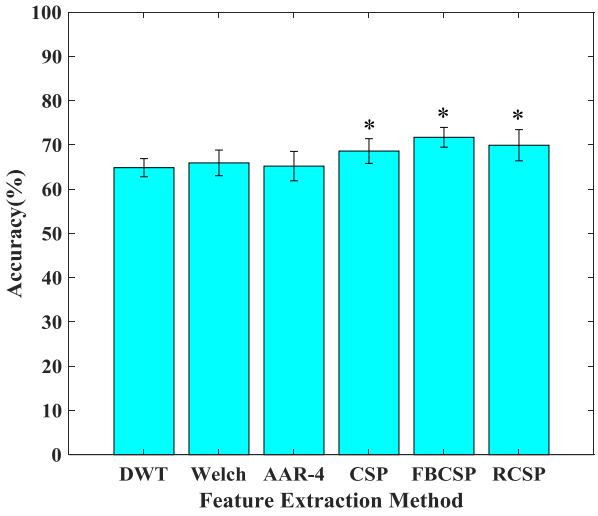

Fig. 5. The average performance (mean ± standard deviation) of different feature extraction methods across eight subjects.

Six feature extraction methods (DWT, Welch, AAR-4, CSP, FBCSP, and RCSP) were individually applied for the eight subjects' datasets. The extracted features were fed to the SVM classifiers. The classification accuracy of SVM with six types of feature datasets were show in Fig. 4. It illustrates that the CSP, FBCSP, and RCSP methods have higher performance for each subjects compared to the DWT, Welch, and AAR-4 methods. More specifically, the average classification performance (mean ± standard deviation) for each feature extraction method is presented in Fig. 5. The DWT, Welch, AAR-4, CSP, FBCSP, and RCSP methods achieved an average accuracy of 64.86 ± 2.05%, 65.95 ± 2.90%, 65.22 ± 3.32%, 68.63 ± 2.79%, 71.73 ± 2.24%, 69.94 ±3.59% respectively. The

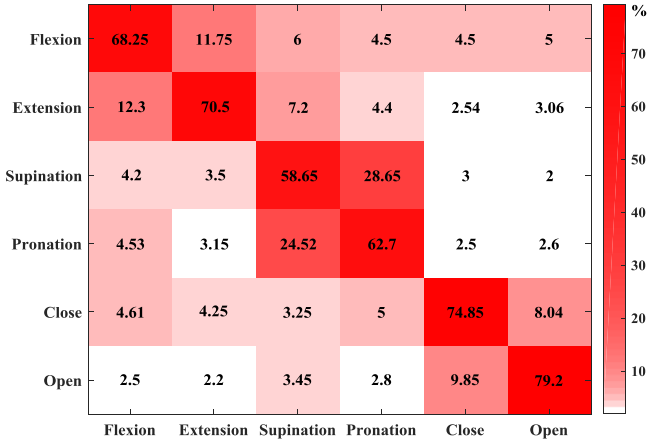

Fig. 6. The accuracy confusion matrix for six classes of MI tasks obtained by SVM classifier with FBCSP methods.

analysis of variance (ANOVA) was carried out to show the statistically significant difference of six methods. The DWT, Welch, and AAR-4 methods have no significant difference (p-value > 0.76) in mean accuracy. However, there is a significant difference (p-value < 0.05) using Kruskal-Wallis test between DWT, Welch, AAR-4 and CSP, FBCSP, RCSP. Especially, the FBCSP method has the best classification accuracy with lower deviation (p-value < 0.01). This result might be attributed to the improved spatial separability of the FBCSP algorithm.

Furthermore, Fig. 6 shows an accuracy confusion matrix obtained by SVM classifier with FBCSP, corresponding to joint movements-level classification results for six MI tasks. The average accuracy was 68.25%, 70.5%, 58.65%, 62.70%, 74.85%, and 79.20% for flexion/extension (elbow joint), supination/pronation (elbow and wrist joint), and close/open (hand), respectively. Interestingly, the distribution of misclassification rates is obviously different for each pair MI tasks. Particularly, the classification accuracies for supination/pronation MI tasks were lower with notable misclassification errors than that of other MI tasks. The possible reason may be the fact that the supination/pronation MI tasks derived from multiple joints within the same limb are closely emerged on the adjacent motor cortex and the spatial separability of the relevant EEG signals is ambiguous.

B. Comparison between LDA and SVM

Moreover, for the features extracted by the FBCSP methods, the comparison analysis of LDA and SVM classifiers were conducted. The accuracies of the two classifiers for each individual and mean accuracies are presented in Fig. 7. Generally, the performance of the SVM is slightly better that that of LDA for each subject. The mean accuracy is 69.02% (± 1.65%) for LDA and 71.78% (± 1.92%) for SVM. The post hoc test using the Kruskal-Wallis method indicates a statistically significant difference in classification accuracy between LDA and SVM, with p-value = 0.012 < 0.05. The increased performance of SVM classifier is benefited by the improved generalization capabilities and maximized separable margins using optimal parameters.

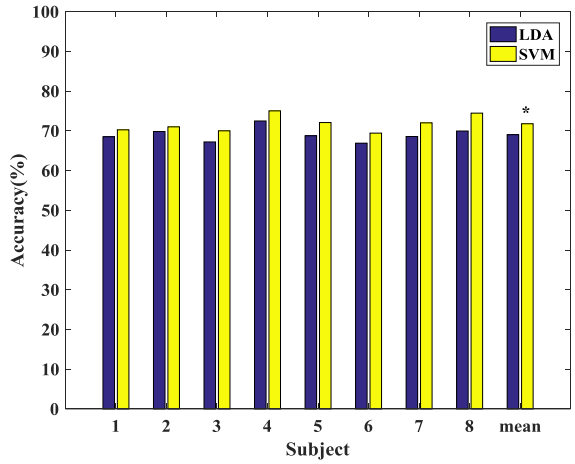

Fig. 7. The accuracy of LDA and SVM classifier for eight subjects.

VI. Conclusions and Future Works

In this paper, we carried out a comparative study for decoding six motor imagery EEG within the same upper extremity by using four types of feature extraction methods and two classifiers (LDA and SVM), including wavelet transformation, power spectrum, AR model, and CSP (FBCSP, RCSP). The CSP algorithm was better than the other three methods, especially for the FBCSP and RCSP methods. Compared to the LDA, the use of the SVM was shown to be suitable for decoding various MI tasks within the same limb. For flexion/extension, supination/pronation, and open/close MI tasks, the highest overall performance of the SVM with FBCSP was obtained, with accuracy of 71.78% (± 1.92%). The obtained results are promising. In the future work, the decoding method can potentially be applied in BCI-driven assistive robots or neuroprosthetics by using natural and intuitive motor imagery EEG signals.

Acknowledgments

This work was supported by the Nation Natural Science Foundation of China (Grants nos. 61503374 and 61573340), and in part by the Frontier Science research project of the Chinese Academy of Sciences (Grant No. QYZDY-SSW-JSC005). The authors would like to thank Yingli Li *et al.* for participating this study.

References

[1] S. Gao, Y. Wang, X. Gao, and B. Hong, "Visual and auditory brain–computer interfaces," *IEEE Trans. Biomed. Eng.*, vol. 61, no. 5, pp.1436-1447, 2014

[2] L. R. Hochberg, D. Bacher, B. Jarosiewicz, N. Y Masse, J. D. Simeral, J. Vogel, *et al.*, "Reach and grasp by people with tetraplegia using a neurally controlled robotic arm," *Nature*, vol. 485, pp. 372-375, 2012

[3] H. Yuan and B. He, "Brain–computer interfaces using sensorimotor rhythms: current state and future perspectives," *IEEE Trans. Biomed. Eng.*, vol. 61, no. 5, pp.1425-1435, 2014

[4] B. He, B. Baxter, B. J. Edelman, C. C. Cline, and Wenjing W. Ye, "Noninvasive brain-computer interfaces based on sensorimotor rhythms," *Proc. IEEE*, vol. 103, no. 6, pp. 907-925, 2015

[5] G. Pfurtscheller, C. Brunner, A. Schlögl, and F. Lopes da Silva, "Mu rhythm (de)synchronization and EEG single-trial classification of different motor imagery tasks," *NeuroImage*, vol. 31, no. 1, pp. 153–9, 2006

[6] J. Wagner, S. Makeig, M. Gola, C. Neuper, and G. R. Müller-Putz, "Distinct β band oscillatory networks subserving motor and cognitive control during gait adaptation," *J. Neurosci.*, vol. 36, pp. 2212–2226, 2016

[7] X. Zhao, Y. Chu, J. Han, and Z. Zhang, "SSVEP-based brain-computer interface controlled functional electrical stimulation system for upper extremity rehabilitation," *IEEE Trans. Syst. Man, Cybern. Syst.*, vol. 46, pp. 947-956, 2016

[8] G. Reshmi, and A. Amal, "Design of a BCI System for Piloting a Wheelchair Using Five Class MI Based EEG," In: *2013 Third International Conference on Advances in Computing and Communications (ICACC)*, pp. 25-28, 2013

[9] Y. N. Li, X. D. Zhang, and Z. X. Huang, "A practical method for motor imagery based real-time prosthesis control," In: *2012 IEEE International Conference on Automation Science and Engineering*, Seoul, pp. 1052–1056, 2012

[10] Y. Chae, J. Jeong, and S. Jo, "Toward brain-actuated humanoid robots: asynchronous direct control using an EEG-based BCI," *IEEE Trans. Robotics*, vol. 28, no. 5, pp. 1131–1144, 2012

[11] D. Coyle, J. Garcia, A. R. Satti, and T. M. McGinnity, "EEG-based continuous control of a game using a 3 channel motor imagery BCI: BCI game," In: *2011 IEEE Symposium on Computational Intelligence, Cognitive Algorithms, Mind, and Brain (CCMB)*, Paris, 2011

[12] T. Geng, M. Dyson, C. S. Tsui, and J. Q. Gan, "A 3-class asynchronous BCI controlling a simulated mobile robot," In: *2007 IEEE Conference on Proceedings of the Engineering in Medicine and Biology Society (EMBS)*, Lyon, pp. 2524-2527, 2007

[13] E. B. Plow, P. Arora, M. A. Pline, M. T. Binenstock, and J. R. Carey, "Within-limb somatotopy in primary motor cortex—revealed using fMRI," *Cortex*, vol. 46, no. 3, pp. 310-321, 2010

[14] X. Yong, and C. Menon, "EEG classification of different imaginary movements within the same limb," *PLoS One*, vol. 10, e0121896, 2015

[15] A. Vuckovic, and F. Sepulveda, "Delta band contribution in cue based single trial classification of real and imaginary wrist movements," *Med. Biol. Eng. Comput.*, vol. 46, no. 6, pp. 529-539, 2008

[16] A. Vuckovic, and F. Sepulveda, "A two-stage four-class BCI based on imaginary movements of the left and the right wrist," *Med. Eng. Phys.*, vol. 34, no. 7, pp. 964-971, 2012

[17] B. J. Edelman, B. Baxter, and B. He, "EEG source imaging enhances the decoding of complex right-hand motor imagery tasks," *IEEE Trans. Biomed. Eng.*, vol. 63, no. 1, pp. 4-14, 2016

[18] K. Liao, R. Xiao, J. Gonzalez, and L. Ding, "Decoding individuals finger movements from one hand using human EEG signals," *PLoS One*, vol. 9, no. 1, e85192, 2014

[19] M. Tavakolan, Z. Frehlick, X. Yong, and C. Menon, "Classifying three imaginary states of the same upper extremity using time-domain features," *PLoS One*, vol. 12, no. 3, e0174161, 2017

[20] P. Ofner, A. Schwarz, J. Pereira, and G. R. Müller-Putz, "Upper limb movements can be decoded from the time-domain of low-frequency EEG," *PLoS One*, vol. 12, no. 8, e0182578, 2017

[21] F. Lotte, L. Bougrain, A. Cichocki, M. Clerc, M. Congedo, A. Rakotomamonjy, *et al.*, "A review of classification algorithms for EEG-based brain-computer interfaces: a 10 year update," *J. Neural Eng.*, vol. 15, no. 3, 031005, 2018

[22] R. V. Wankar, P. Shah, and R. Sutar, "Feature extraction and selection methods for motor imagery EEG signals: A review," In: *2017 International Conference on Intelligent Computing and Control (I2C2)*, Coimbatore, pp. 1-9, 2017

[23] P. Herman, G. Prasad, T. M. McGinnity, and D. Coyle, "Comparative analysis of spectral approaches to feature extraction for EEG-based motor imagery classification," *IEEE Trans. Neural Syst. Rehabil. Eng.*, vol. 16, no. 4, pp. 317-326, 2008

[24] R. Yang, A. Song, and B. Xu, "Feature extraction of motor imagery EEG based on wavelet transform and higher-order statistics," *Int. J. Wavelets Multiresolut. Inf. Process.*, vol. 8, no. 3, pp. 373-384, 2010

[25] K. Inoue, D. Mori, G. Pfurtscheller, and K. Kumamaru, "Pattern recognition of EEG signals during right and left motor imagery," *Complex Medical Engineering*, Springer, Tokyo, pp. 251-261, 2007

[26] Y. Zhang, G. Zhou, J. Jin, X. Wang, and A. Cichochi, "Optimizing spatial patterns with sparse filter bands for motor-imagery based brain-computer interface," *J. Neurosci. Methods*, vol. 255, pp. 85-91, 2015

[27] A. Delorme and S. Makeig, "EEGLAB: an open source toolbox for analysis of single-trial EEG dynamics," *J. Neurosci. Methods*, vol. 134, no. 1, pp. 9-21, 2004